Reprinted from

JOURNAL OF THE PHYSICAL SOCIETY OF JAPAN

JOURNAL OF THE PHYSICAL SOCIETY OF JAPAN

http://jpsj.jpap.jp/

FULL PAPER

Pump–probe and Four-wave Mixing Spectra Arising from Recoil-induced Resonance in an Operating Cesium Magneto-Optical Trap

Zhonghua Ji, Hongshan Zhang, Dianqiang Su,
Yanting Zhao, Liantuan Xiao, and Suotang Jia

J. Phys. Soc. Jpn. **87**, 024301 (2018)

Journal of the Physical Society of Japan **87**, 024301 (2018)
https://doi.org/10.7566/JPSJ.87.024301

Pump–probe and Four-wave Mixing Spectra Arising from Recoil-induced Resonance in an Operating Cesium Magneto-Optical Trap

Zhonghua Ji[1,2], Hongshan Zhang[1,2], Dianqiang Su[1,2], Yanting Zhao[1,2*], Liantuan Xiao[1,2], and Suotang Jia[1,2]

[1]*State Key Laboratory of Quantum Optics and Quantum Optics Devices, Institute of Laser Spectroscopy, Shanxi University, Taiyuan, Shanxi 030006, China*
[2]*Collaborative Innovation Center of Extreme Optics, Shanxi University, Taiyuan, Shanxi 030006, China*

(Received August 6, 2017; accepted November 30, 2017; published online December 27, 2017)

We present experimental observation of recoil-induced resonance (RIR) in an operating cesium magneto-optical trap (MOT) by both pump–probe absorption and four-wave mixing spectra simultaneously. We investigate the dependence of amplitudes of these two spectra on pump beam intensity and frequency. The measurement results agree well with the recoil-induced theory with modifications of Raman transition effect and atomic number. The systematical study on RIR spectra is meaningful for the diagnostic measurement of cold atoms in an operating MOT.

1. Introduction

Laser cooling and trapping of neutral atoms have been widely used in physics research.[1)] When an atom interacts with a photon, there is a corresponding change in the atom's center-of-mass momentum due to momentum conservation. The momentum exchange is associated with a phenomenon called recoil-induced resonance (RIR) which was predicted first by Guo et al.[2)] The authors calculated the resonance line shape for an ensemble of two-level atoms interacting with laser fields in a pump–probe or four-wave mixing (FWM) geometry. The spectra exhibit rich structures with typical linewidths on the order of 10–100 kHz.

Pump–probe spectroscopy[3)] as a non-destructive, highly sensitive diagnostic tool can be used to extract information on specific samples. Researchers use this technique to investigate molecular dynamics[4)] and nanoscale composite,[5)] predict coherent evolution of a quantum system[6)] and measure light shift of ultracold atoms.[7)] Four-wave mixing is an effective way to generate correlations and entanglements in quantum optics.[8,9)] The simultaneous requirements of conservation of energy and momentum in the process facilitate the appearance of quantum coherence. Also, FWM can be used for temperature diagnostics,[10)] wavelength conversion and parametric amplification.[11)]

The earliest experiments on RIR absorption spectroscopy of cold trapped atoms were carried out in cesium (Cs) magneto-optical trap (MOT) where the counter propagating laser beams play the role of both cooling and pump lights.[12,13)] Furthermore, Gordon et al. have proposed and explored the possibility in utilizing the RIR structure as an optical switch.[14)] Vengalattore et al. created a slow-light optical waveguide with the strong dispersion and large gain in the RIR regime.[15)] Lasing was also demonstrated in the RIR gain medium.[16)]

The MOT is an useful tool for producing large numbers of atoms at sub-mK temperature. This method not only increases the atomic density and decreases the collision rate, but also reduces Doppler broadening and enhances optical nonlinearity. In an operating MOT, RIR spectrum can constitute a powerful, nondestructive diagnostic tool. For examples, it can provide information on the atomic energy level shift,[17)] atomic temperature,[18)] momentum distribution,[19–21)] nonlinear coherent interaction.[22)] Thus a RIR spectra with good signal-to-noise (SNR) is helpful for these applications.

In this paper, we simultaneously present pump–probe absorption spectrum and four-wave mixing spectrum arising from RIR in an operating Cs MOT. To simulate the observed spectrum, a previous recoil-induced theory with addition of Raman transition effect is applied in these two kinds of spectroscopy. To optimize the amplitude of RIR spectrum, we measure the influence of the intensity and frequency of pump beam on the RIR spectra. A agreement between experimental measurement and theory is observed after a modification of cold atomic number which is influenced by pump beam. The study will be meaningful for the diagnostic measurement of cold atoms in an operating MOT.

2. Theoretical Description

The RIR phenomenon comes from the momentum exchange between the interacting atoms and light fields.[2,23)] We assume the atom with mass M interacts with a strong pump beam with wave vector k and a weak probe beam with wave vector k_p. There is a small angle θ between the pump and probe beams. Assuming the probe beam frequency detuning δ (defined as $\delta = f_{\text{probe}} - f_{\text{pump}}$, where f_{probe} and f_{pump} are frequencies of probe and pump beam respectively) is sufficiently small, one finds that $|k_p| \approx |k| = k$. As shown in Fig. 1, when $\delta < 0$, the atom absorbs a pump photon and then emits a probe photon. This is a gain process, resulting in the atom momentum change by $\Delta p = -\hbar k\theta$, where $\hbar$ is the reduced Planck constant. Similarly, when $\delta > 0$, the atom absorbs a probe photon and then emits a pump photon. This is an absorption process, resulting in the atom momentum change by $\Delta p = \hbar k\theta$. The amplitude of the resonance structure is proportional to the population difference $\Pi(p + \Delta p) - \Pi(p)$, where $\Pi(p)$ is Gaussian distribution of atomic momentum.

Considering continuum momentum distribution and integrating over all possible values of atomic momentum, the amplitude coefficient of probe field induced by RIR[2,24)] can be written as

$$g_{\text{RIR}}(\delta) = \frac{\Omega^2\Omega_p}{\Delta^2}\int dp\,\frac{\gamma(\Pi(p+\hbar k\theta) - \Pi(p))}{\gamma^2 + (\delta - k\theta p/M)^2}, \qquad (1)$$

where Ω and Ω_p are the resonance Rabi frequencies of the pump beam and probe beam, respectively. Δ is the frequency

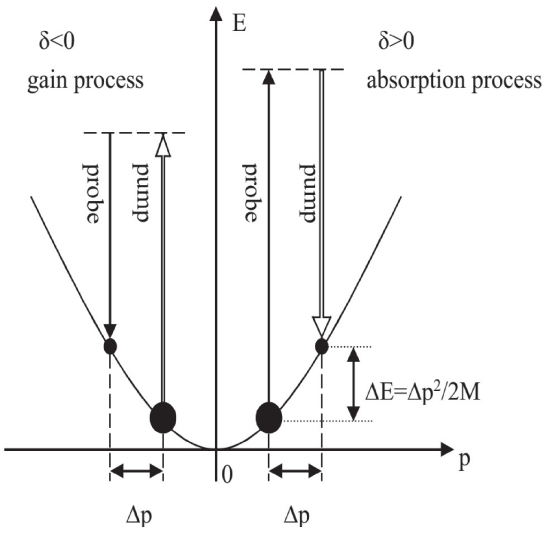

Fig. 1. The scheme of atomic energy and momentum changes in an operating MOT. The gain process corresponds to $\delta < 0$ and absorption process corresponds to $\delta > 0$. The black circles symbolize populations $\Pi(p)$ of corresponding kinetic states.

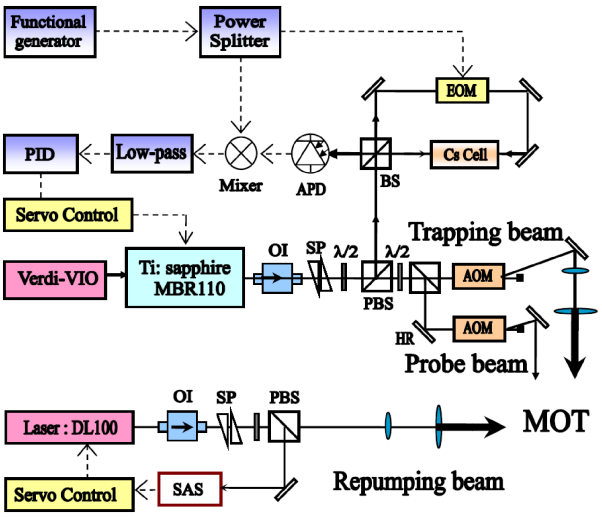

Fig. 2. (Color online) The optical scheme of the experiment. PBS: polarization beam splitter; APD: avalanche photodiode; BS: beam splitter; PID: proportion integral differential circuit; OI: optical isolator; SP: shaping prism; SAS: saturated absorption spectrum. The dashed lines represent electric signals, and the solid lines represent optical paths.

detuning of pump beam from the atomic resonance, and γ is the population relaxation rate. Assuming that $\gamma \ll k\overline{v}\theta$, where $\overline{v} = p/M$ is the mean atomic velocity, one obtains an analytic formula

$$g_{\mathrm{RIR}}(\delta) = \sqrt{\frac{\pi}{2}}\frac{\hbar\Omega^2\Omega_P}{\Delta^2 k_{\mathrm{B}}T}\left\{\frac{3}{20}\left(\frac{1}{\Delta}\int \exp\left[-\frac{\delta^2}{2(k\theta\overline{v})^2}\right]dx - \frac{\hbar k}{m\overline{v}}\left(\frac{\delta}{k\theta\overline{v}}\right)^2 \exp\left[-\frac{\delta^2}{2(k\theta\overline{v})^2}\right]\right) - i\frac{\delta}{k\theta\overline{v}}\exp\left[-\frac{\delta^2}{2(k\theta\overline{v})^2}\right]\right\}, \quad (2)$$

where k_{B} is Boltzmann constant, and T is the temperature of the atomic sample.

The pump–probe spectrum (RIR signal in absorption spectrum) is quantitatively described by imaginary part of Eq. (2) $\mathrm{Im}[g_{\mathrm{RIR}}(\delta)]$. The resonance structure is a derivative of Gaussian function at $\delta = 0$. The FWM spectrum is background free, hence RIR signal in FWM spectrum appear much more sensitive to the weak recoil effects than the case of corresponding absorption signal. It is proportional to $|g_{\mathrm{RIR}}(\delta)|^2$.[2] The resonance structure has an ultra-narrow feature at $\delta = 0$, which is due to the transitions between kinetic momentum states correlated to the Rayleigh scattering.

For cold atoms in MOT, the pump–probe spectrum arising from RIR has be modified by contribution of Raman signal, which contains the roles of different magnetic sublevels.[23] Raman signal can be calculated under a semi-classical treatment where the atomic center-of-mass momentum and position are treated as classical variables. After solving the atomic density-matrix elements from generalized optical Bloch equations and considering the low-field intensity and low-energy approximations, one can get an equation for the Raman signal

$$g_{\mathrm{Rm}}(\delta) = \frac{25}{1224}\frac{i\Omega^2\Omega_p}{\gamma + i\Delta}\left\{\frac{1}{5\Gamma/6 + i\delta}\frac{1}{\gamma - i\Delta} + \frac{1 - \dfrac{\Gamma'/15}{5\Gamma/6 + i\delta}\dfrac{i\Delta}{\Gamma}}{\dfrac{\Gamma'}{6} + i\delta + \dfrac{(\Gamma'/3)^2(\Delta/\Gamma)^2}{5\Gamma'/6 + i\delta}}\left[3 - \frac{2\Gamma'/3}{5\Gamma/6 + i\delta\Gamma}\frac{i\Delta}{\Gamma} + \frac{2}{\gamma + i(\Delta + \delta)}\right]\right\}. \quad (3)$$

Where $\Gamma' = \Gamma|\Omega|^2/[(\Gamma/2)^2 + \Delta^2]$ is the effective decay rate of each sub-level. Due to the effect of the Raman transition background, the overall signal of pump–probe absorption spectrum has been modified to $\mathrm{Im}[g_{\mathrm{Rm}}(\delta)] + \mathrm{Im}[g_{\mathrm{RIR}}(\delta)]$, and the overall RIR four-wave mixing signal should be modified to $|g_{\mathrm{Rm}}(\delta) + g_{\mathrm{RIR}}(\delta)|^2$.

3. Experimental Setup

The setup of our experiment is depicted in Fig. 2. The Cs atoms are trapped in a MOT with a vacuum environment (about 3×10^{-7} Pa). Both trapping beam and probe beam come from a Ti:sapphire laser (Coherent, MBR110). The frequency detuning of the trapping beam is fixed at $\Delta = -3\Gamma$ (Γ is the natural linewidth of Cs $D2$ line) from the atomic resonant transition of the $6S_{1/2}(F = 4) \rightarrow 6P_{3/2}(F' = 5)$ using an acousto-optic modulator (AOM). A Littman–Metcalf external-cavity diode laser (Toptica DL100) is used as repumping beam, whose output power is 2 mW and frequency is stabilized to the resonant transition of the $6S_{1/2}(F = 3) \rightarrow 6P_{3/2}(F' = 4)$ by saturated absorption spectroscopy (SAS). A pair of anti-Helmholtz coils generates 15 G/cm magnetic field gradient. We can trap about 5×10^7 atoms with a temperature of about 85 μK, which is measured by time-of-flight absorption imaging.

The trapping beam is divided into three pairs of mutually orthogonal laser beams with opposite $\sigma^{+/-}$ polarizations. We choose one of the trapping beams (x-direction) as the pump beam. The probe beam injects into the sample at a small

angle $\theta = 2^\circ$ relative to this pump beam. The polarization of the probe beam is σ^- polarized, controlled by a $\lambda/4$ waveplate. The arrangement of polarizations of probe beam and pump beams are the same as Ref. 23. Typically, the waist of probe beam is about 1 mm while the power is 12 μW, which cannot destruct the atomic cloud. The probe beam is recorded by an avalanche photodiode (APD) after going through the cold sample, and the four-wave mixing signal is retro-reflected from the cold sample and recorded simultaneously by another APD. The spatial position of FWM signal is determined by phase-conjugation of probe beam, satisfying momentum conservation. Only the probe beam irradiates the cold atoms, we can observe the FWM signal on the desired position. In order to detect sub-MHz narrow multiphoton resonances, the probe beam used for RIR spectroscopy is split off from the pump beam, that provides the necessary phase coherence. Thus, the pump–probe absorption spectrum after interacting with the cold sample has a high resolution, which allows us to distinguish the RIR signal with the order of kHz width.

4. Experimental Results

We scan the probe beam frequency by changing the radio frequency of AOM and record the intensities of two APDs simultaneously to obtain the pump–probe and FWM spectra, respectively. As the scanning frequency range of AOM is very narrow (sub-MHz), the variation of probe beam position can be ignored. Figures 3(a) and 3(c) separately show the RIR absorption spectrum and the FWM spectrum as a function of probe beam detuning δ. The spectra contain two parts, the broad one is the Raman transition structure and the narrow one is RIR signal resulting from the interaction between the probe beam and the pump beams with atoms.

Figures 3(b) and 3(d) are enlarged views of Figs. 3(a) and 3(c), respectively. Figure 3(b) shows the dispersion-like RIR absorption spectrum near $\delta = 0$. Here, we define the difference of peak–peak values as the amplitude of RIR absorption spectrum. Figure 3(d) shows the four-wave mixing spectrum of RIR with an apparent dip near $\delta = 0$. We define the difference between the minimum value and background as the amplitude of RIR FWM spectrum. The dashed line and dot line in Fig. 3(b) represent the simulated results by $\mathrm{Im}[g_{\mathrm{RIR}}(\delta)]$ and $\mathrm{Im}[g_{\mathrm{RIR}}(\delta)] + \mathrm{Im}[g_{\mathrm{Rm}}(\delta)]$, respectively. We can see that the absorption spectrum agree well with the latter one, which contains the contribution of Raman background. Analogously, the dashed line and dot line in Fig. 3(d) represent the simulated results by $|g_{\mathrm{RIR}}(\delta)|^2$ and $|g_{\mathrm{RIR}}(\delta) + g_{\mathrm{Rm}}(\delta)|^2$, respectively. It also shows that the FWM spectrum also agree well with the latter one. Our measurements show that Raman transition only affects the absorption signal at two sides and has little influence near resonance while it results in the asymmetry for the FWM signal near resonance, comparing absorption spectrum.

To obtain RIR spectra with good SNR, we optimize the pump beam intensity and frequency for these two kinds of spectra. Figures 4(a) and 4(b) show the relationships between the amplitude of pump–probe spectrum versus the pump beam intensity and frequency detuning (relative to $\Delta = -3\Gamma$) respectively. According to Eq. (2), one would expect that the amplitude of pump–probe spectrum is proportional to the intensity of pump beam and inversely proportional to the square of pump beam detuning, which are shown with dot lines. However, we observe a saturated effect with the pump beam intensity as shown in Fig. 4(a) and one maximum value

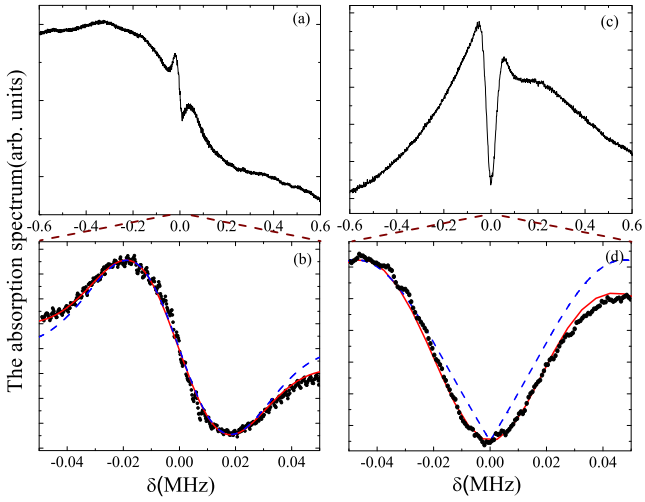

Fig. 3. (Color online) The pump–probe (a) and the four-wave mixing spectrum (c) based on the recoil induced resonance. The spectra are recorded as a function of the probe beam detuning δ. (b) and (d) are enlarged views of (a) and (c), respectively. The dashed line and dot line in (b) represent the simulated results by $\mathrm{Im}[g_{\mathrm{RIR}}(\delta)]$ and $\mathrm{Im}[g_{\mathrm{RIR}}(\delta)] + \mathrm{Im}[g_{\mathrm{Rm}}(\delta)]$, respectively. Analogously, the dashed line and dot line in (d) represent the simulated results by $|g_{\mathrm{RIR}}(\delta)|^2$ and $|g_{\mathrm{RIR}}(\delta) + g_{\mathrm{Rm}}(\delta)|^2$, respectively. The intensity of the pump beam is 25 mW/cm^2 and the probe beam is fixed at 12 μW and the detuning of the pump beam is $\Delta = -3\Gamma$. The magnetic gradient is 15 G/cm and the angle is $\theta = 2^\circ$.

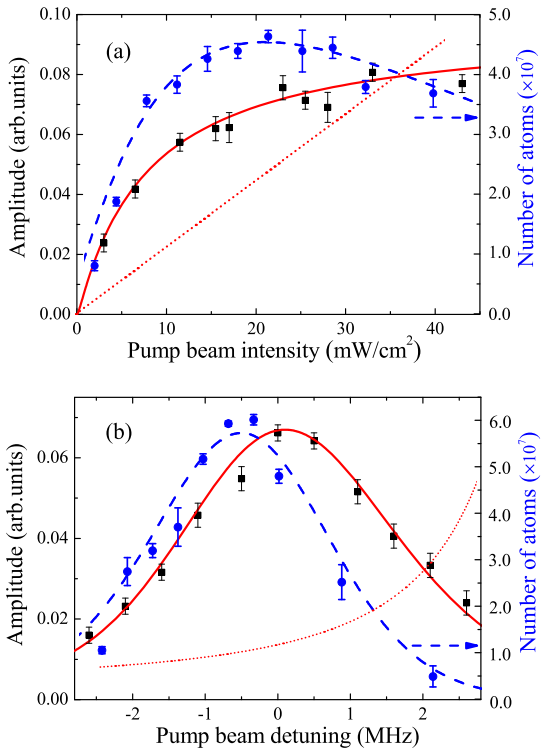

Fig. 4. (Color online) The amplitude of the RIR signals in absorption spectrum versus the pump beam intensity (a) and detuning (b). The detuning in (a) and the intensity in (b) are -3Γ and 25 mW/cm^2 respectively. The dashed lines are the relations between the atomic numbers and pump beam intensity and detuning respectively. The dot (solid) lines are the calculated amplitudes of the RIR absorption signals by RIR theory without (with) modification of Raman contribution and atomic number.

with pump frequency detuning as shown in Fig. 4(b). We attribute these deviations to the influence of the number of cold atoms when we change the pump beam intensity and frequency. Thus, we measure the atomic number, which are shown with circle points in Fig. 4. To add the influence of atomic number to the RIR theory, a theoretical expression of atomic number is also needed besides of the experimental measurement. Based on Ref. 25, the number of trapped atoms can be written as

$$N = 0.1\frac{A}{\sigma}\left(\frac{\nu_c}{\nu_{\text{thermal}}}\right)^4. \tag{4}$$

Where A is the surface area of the trapping region assuming that the region is spherical with the beam diameter, the cross section σ for a normal MOT is about $1.5 \times 10^{-9}\,\text{cm}^{-2}$,[26] ν_c is the maximum velocity of an atom can be captured, and $\nu_{\text{thermal}} = 193\,\text{m/s}$ is the average velocity of the background gas. This equation is widely used by other groups and the reliability has been verified.[27,28] Ignoring the effects of magnetic field and the Gaussian intensity profile of the laser beams, the radiation pressure force can be written as[25]

$$F = \frac{\hbar k'\Gamma}{2}\frac{I}{I_{\text{sat}}}\left(\frac{1}{1+\frac{I}{I_{\text{sat}}}+4\left(\frac{2\pi\Delta}{\Gamma}-\frac{k'\nu}{\Gamma}\right)^2} - \frac{1}{1+\frac{I}{I_{\text{sat}}}+4\left(\frac{2\pi\Delta}{\Gamma}+\frac{k'\nu}{\Gamma}\right)^2}\right). \tag{5}$$

Where I is the trapping beam intensity, I_{sat} is the atomic saturation intensity, k' is the wave number of the trapping beam, and ν is the trapped atomic velocity. ν_c can be obtained by solving the equation of motion using the Eq. (5). Combining Eq. (4) with Eq. (5), we can obtain the relationships between the atomic number and the pump beam intensity and frequency detuning, shown with dashed lines in Fig. 4. After modification of atomic number and Raman transition to Eq. (2), we then get the theoretical fitting curve [the dot lines in Figs. 4(a) and 4(b)], which agrees well with experimental measurements (black squares).

Figures 5(a) and 5(b) show the relationship between the amplitude of four-wave mixing signal versus the pump beam intensity and frequency detuning, respectively. Analogously, if we do not consider modification of Raman contribution and atomic number, one would expect that the amplitude of the RIR four-wave mixing signal should be proportional to the square of the pump beam intensity, and inversely proportional to the quadruplicate power of the pump beam frequency detuning, which are shown with dot lines. However, we observe a nearly linear relationship with the pump beam intensity as shown in Fig. 5(a), and one maximum value with pump frequency detuning as shown in Fig. 5(b). It is noticed that the amplitude dependence of four-wave mixing in Fig. 5(b) is obvious asymmetry compared with RIR signals in Fig. 4(b). The dashed lines in Fig. 5 are the same as the ones in Fig. 4. The dot lines are the theoretical fitting curves after modification of atomic number and Raman contribution, then we find that it match well with experimental results.

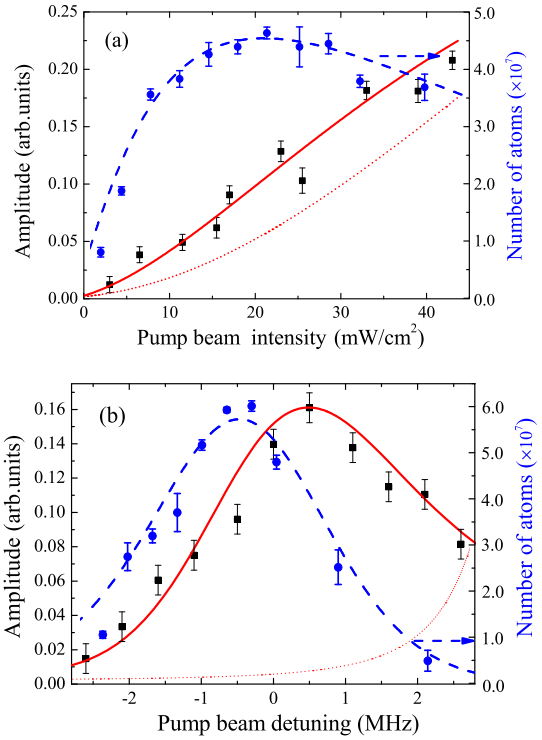

Fig. 5. (Color online) The amplitude of the RIR four-wave mixing signals versus the pump beam intensity (a) and detuning (b). The conditions of experiments are the same as the ones in Fig. 4. The dot (solid) lines are the calculated amplitude of the RIR four-wave mixing signals by RIR theory without (with) modification of Raman contribution and atomic number.

5. Conclusions

We have observed the pump–probe and four-wave mixing spectra arising from recoil-induced resonance in an operating MOT simultaneously. To simulate the observed spectra, a recoil-induced theory with Raman transition contribution is applied to both absorption spectrum and FWM spectra. We find that the Raman transition only affects the RIR absorption signal at two sides and has little influence on the width and amplitude near resonance. Contrastively, the Raman transition effect results in the asymmetry for the RIR four-wave mixing signal. We investigate the dependence of the amplitudes of these two spectra on the pump beam intensity and frequency. To overcome the deviation between measured relationships and the RIR theory, we take into account the effect of atomic number and Raman contribution, then get a good agreement between the theoretical simulation and experiment. Our study on RIR spectra is meaningful for the diagnostic measurement of cold atoms in an operating MOT.

Acknowledgements The work is supported by National Key R&D Program of China (Grant No. 2017YFA0304203), Natural Science Foundation of China (Nos. 61675120, 11434007, and 61378015), NSFC Project for Excellent Research Team (No. 61121064), Shanxi Scholarship Council of China, PCSIRT (No. IRT 13076) and Applied Basic Research Project of Shanxi Province (No. 201601D202008).

*zhaoyt@sxu.edu.cn

1) W. D. Phillips, Rev. Mod. Phys. **70**, 721 (1998).
2) J. Guo, P. R. Berman, B. Dubetsky, and G. Grynberg, Phys. Rev. A **46**, 1426 (1992).
3) F. Y. Wu, S. Ezekiel, M. Ducloy, and B. R. Mollow, Phys. Rev. Lett. **38**, 1077 (1977).

4) Y. Mairesse, S. Haessler, B. Fabre, J. Higuet, W. Boutu, P. Breger, E. Constant, D. Descamps, E. Mével, S. Petit, and P. Salières, New J. Phys. **10**, 025028 (2008).
5) T. Virgili, G. Grancini, E. Molotokaite, I. Suarez-Lopez, S. K. Rajendran, A. Liscio, V. Palermo, G. Lanzani, D. Polli, and G. Cerullo, Nanoscale **4**, 2219 (2012).
6) S. Maneshi, C. Zhuang, C. R. Paul, L. S. Cruz, and A. M. Steinberg, Phys. Rev. Lett. **105**, 193001 (2010).
7) N. Souther, R. Wagner, P. Harnish, M. Briel, and S. Bali, Laser Phys. Lett. **7**, 321 (2010).
8) C. Shu, X. Guo, P. Chen, M. M. T. Loy, and S. Du, Phys. Rev. A **91**, 043820 (2015).
9) Y. Fang, Z. Qin, H. Wang, L. Cao, J. Xin, J. Feng, W. Zhang, and J. Jing, Sci. China Phys. Mech. Astron. **58**, 1 (2015).
10) M. Mitsunaga, M. Yamashita, M. Koashi, and N. Imoto, Opt. Lett. **23**, 840 (1998).
11) S. Lavdas, S. Zhao, J. B. Driscoll, R. R. Grote, R. M. Osgood, and N. C. Panoiu, Opt. Lett. **39**, 4017 (2014).
12) J. W. R. Tabosa, G. Chen, Z. Hu, R. B. Lee, and H. J. Kimble, Phys. Rev. Lett. **66**, 3245 (1991).
13) D. Grison, B. Lounis, C. Salomon, J. Y. Courtois, and G. Grynberg, Europhys. Lett. **15**, 149 (1991).
14) K. Gordon, S. DeSavage, D. Duncan, G. Welch, J. Davis, and F. Narducci, J. Mod. Opt. **57**, 1849 (2010).
15) M. Vengalattore and M. Prentiss, Phys. Rev. Lett. **95**, 243601 (2005).
16) W. Guerin, F. Michaud, and R. Kaiser, Phys. Rev. Lett. **101**, 093002 (2008).
17) Z. Ji, Y. Zhao, J. Ma, L. Xiao, and S. Jia, J. Phys. Soc. Jpn. **81**, 104301 (2012).
18) Y.-T. Zhao, D.-Q. Su, Z.-H. Ji, H.-S. Zhang, L.-T. Xiao, and S.-T. Jia, Chin. Phys. B **24**, 093701 (2015).
19) J. A. Greenberg and D. J. Gauthier, Phys. Rev. A **79**, 033414 (2009).
20) M. Brzozowska, T. M. Brzozowski, J. Zachorowski, and W. Gawlik, Phys. Rev. A **72**, 061401 (2005).
21) M. Brzozowska, T. M. Brzozowski, J. Zachorowski, and W. Gawlik, Phys. Rev. A **73**, 063414 (2006).
22) M. Vengalattore, M. Hafezi, M. D. Lukin, and M. Prentiss, Phys. Rev. Lett. **101**, 063901 (2008).
23) J. Guo and P. R. Berman, Phys. Rev. A **47**, 4128 (1993).
24) J.-Y. Courtois, G. Grynberg, B. Lounis, and P. Verkerk, Phys. Rev. Lett. **72**, 3017 (1994).
25) K. Lindquist, M. Stephens, and C. Wieman, Phys. Rev. A **46**, 4082 (1992).
26) K. E. Gibble, S. Kasapi, and S. Chu, Opt. Lett. **17**, 526 (1992).
27) M. Haw, N. Evetts, W. Gunton, J. V. Dongen, J. L. Booth, and K. W. Madison, J. Opt. Soc. Am. B **29**, 475 (2012).
28) G. W. Hoth, E. A. Donley, and J. Kitching, Opt. Lett. **38**, 661 (2013).